Journal of Molecular Spectroscopy **199,** 100–108 (2000)
Article ID jmsp.1999.7999, available online at http://www.idealibrary.com on IDEAL®

The Near-Infrared Transition of CuCl Observed by Intracavity Laser Spectroscopy

L. C. O'Brien,*[,1] Hong Cao,† and James J. O'Brien†

*Department of Chemistry, Southern Illinois University at Edwardsville, Edwardsville, Illinois 62026-1652; and †Department of Chemistry, University of Missouri-St. Louis, St. Louis, Missouri 63121-4499

Received August 6, 1999; in revised form September 27, 1999

The near-infrared electronic transition of CuCl, occurring in the region of 745 nm, was recorded using intracavity laser absorption spectroscopy. The (0, 0), (1, 1), and (2, 2) vibronic bands were analyzed, and from this the molecular constants for the two electronic states were derived. Originally assigned as $A'\ ^3\Sigma^+–X^1\Sigma^+$, we have confirmed that this transition does not connect to the ground state, but occurs between two unknown excited states. The excited CuCl molecules were produced in a copper hollow cathode, operated using argon and a small amount of CCl_4. Line positions were referenced to iodine spectra observed from a heated extracavity cell using the broadband spectral output of the intracavity laser as the light source.

INTRODUCTION

In 1974 Rao and Rao (*1*) reported a vibrational analysis of a violet-degraded, near-infrared electronic transition of CuCl at 13 500 cm^{-1}. Spectra from isotopically enriched CuCl (^{65}Cu and ^{37}Cl) confirmed that the bands were due to CuCl. They concluded that the lower state of the near-infrared transition probably was the ground state because of the similarity of the ground state vibrational constants with the near-infrared lower state vibrational constants. In 1984 Balfour and Ram (*2*) reported a rotational analysis of the violet-degraded (0, 0) vibronic band, using ground state rotational constants from microwave spectroscopy (*3*). They assigned the near-infrared CuCl transitions as $A'\ ^3\Sigma^+–X^1\Sigma^+$, by analogy with the red $a^3\Sigma^+–X^1\Sigma^+$ transition of CuF (*4*), which also is violet-degraded.

Results from excited state lifetime measurements of the formerly so-called $A^1\Pi$ state at 18 995 cm^{-1} (not to be confused with the newly labeled $A^1\Pi$ state lying at T_0 = 22 958.5 cm^{-1}; see below) of CuCl (*5*) and *ab initio* calculations (*6–9*), however, have led to questions about the electronic state assignments of the visible and near-infrared bands of CuCl. First, the lifetime of the original $A^1\Pi$ state is found to be about 60 μs (*5*), which does not match the calculated lifetime of any $^1\Pi$ state but rather matches the calculated lifetime of the lowest $^3\Sigma_1^+$ state (*7*). Second, theoretical calculations place the electronic energy of the lowest lying $^3\Sigma^+$ state at more than 17 500 cm^{-1} (*6–9*), which more closely matches the energy of the original $A^1\Pi$ state (*10*) than the reported energy for the $A'\ ^3\Sigma^+$ state (*2*). This evidence has led to speculations that the expected low-lying $^3\Sigma^+$ state is not the A' state as originally believed, but rather is the original A state, incorrectly assigned as a $^1\Pi$ state in former studies (*5–9*). This would imply that the near-infrared bands are misassigned and do not connect to the ground state.

The visible transitions of CuCl have been the subject of a recent review by Parekunnel *et al.* (*11*). The review contains a reanalysis of the transitions with the new assignments based on high-level *ab initio* calculations (*6–9*); all of the visible transitions are reassigned in the paper. Parekunnel *et al.* report, in agreement with the *ab initio* calculations, that the first excited electronic state (formerly the $A^1\Pi$ state) is of $a^3\Sigma^+$ symmetry, with the $\Omega = 1$ component lying at about 19 000 cm^{-1}.

Certainly only one low-lying $^3\Sigma^+$ state of CuCl should exist (*6–9*), thus the electronic assignment of the near-infrared band at 13 500 cm^{-1} is questioned. Previously, part of the problem in making a definitive assignment for the near-infrared band has been the inability of several groups to reproduce the near-infrared emission, either to determine the excited state lifetime (*5*) or to record the spectrum at higher resolution (*12*). We have used intracavity laser absorption spectroscopy to record the near-infrared absorption spectrum of CuCl at Doppler-limited resolution.

EXPERIMENTAL DETAILS

Spectra are acquired using a copper hollow cathode contained within the resonator of an intracavity laser spectrometer (ILS) that is based on a Ti:sapphire laser. A schematic of the system is provided in Fig. 1. The spectrometer is fully described by Kalmar and O'Brien (*13*). A briefer coverage follows.

Quantitatively accurate, spectral information for an absorb-

[1] To whom correspondence should be addressed. E-mail: lobrien@siue.edu.

0022-2852/00 $35.00

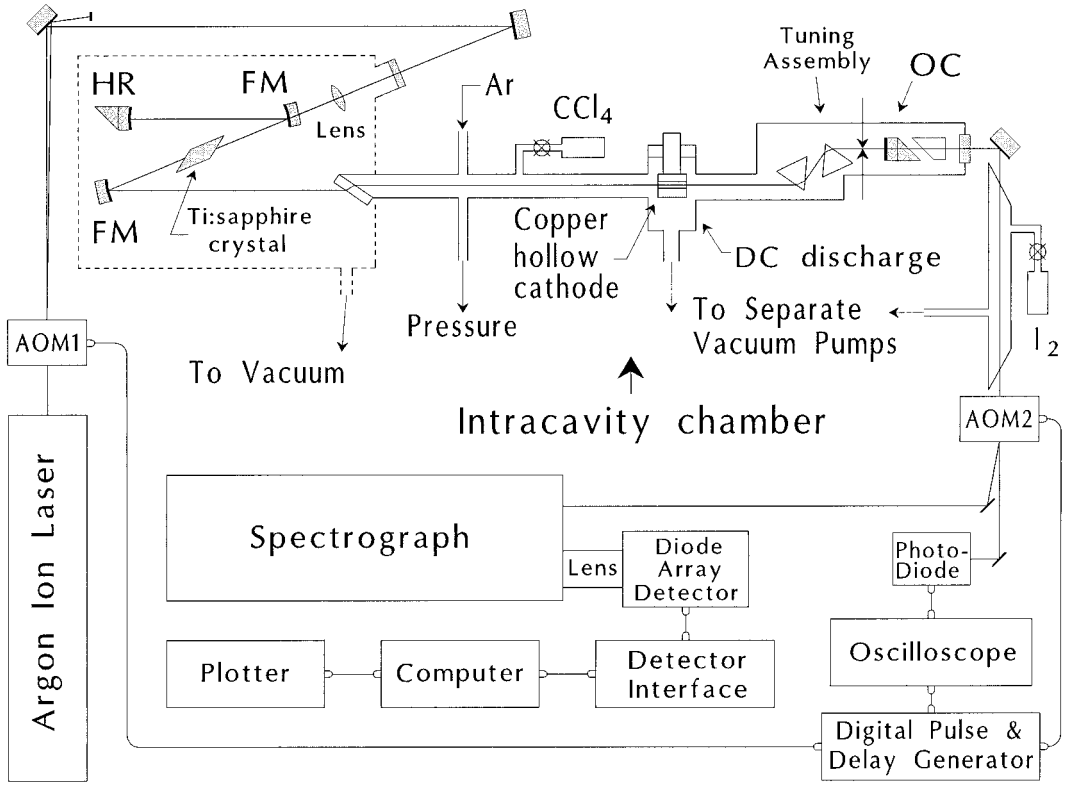

FIG. 1. Schematic diagram for the intracavity laser spectrometer. AOM = acousto-optic modulator; HR = high reflector; FM = fold mirror; OC = output coupler.

ing species in an ILS experiment can be obtained from the time-modulated operation of a homogeneously broadband laser. When the spectral output of a laser operated in this manner is examined with a high-resolution spectrograph, absorption lines of an intracavity species appear superimposed on the spectrally broadband output of the laser. By delaying the observation of the spectral output for a period of time (~100 μs–1 ms) after the onset of laser operation, very high detection sensitivities can be achieved. The time period is termed the generation time, t_g. Enhancement ratios greater than 10^6 have been observed. A specially configured dye laser was used in attaining the highest sensitivity achieved so far; the corresponding effective path length was 70 000 km (*14*).

The observed transmittance, $I_{obs}(\nu)$, at a particular frequency ν, is related to t_g via the equation:

$$I_{obs}(\nu) = I_0(\nu)\exp[-\sigma(\nu)\,N(l/L)ct_g]. \qquad [1]$$

In this equation, $I_0(\nu)$ is the intensity of the laser in the absence of absorption and indicates the 100% transmittance level, $\sigma(\nu)$ is the absorption cross section, N is the number density for the intracavity absorber, l/L is the fraction of the laser cavity of length L occupied by the absorber, and c is the speed of light. The combination $(l/L) \cdot c \cdot t_g$ represents the effective absorption path length, so Eq. [1] expresses the Beer–Lambert relationship for ILS.

The standing wave, four mirror (HR, FM, FM, OC in Fig. 1), Ti:sapphire laser is pumped by all visible lines of an argon ion laser. Spectra are obtained at a specific generation time by the sequential operation of two acousto-optic modulators, AOM1 and AOM2. Modulated operation of AOM1 causes the pump power directed into the laser crystal (Crystal Systems) to be alternatively above and below the threshold value required for laser operation. Activation of AOM2 diverts ~70% of the Ti:sapphire laser output into a high-resolution spectrograph for a time period (~0.1 μs) much shorter than t_g. Dispersed light exciting the spectrograph is focused at a ×3 magnification onto the 1024 channels of a diode-array detector. The sequence is repeated at a 10-kHz rate. Spectral data are collected for five accumulations of 0.6-s scan times using a multichannel analyzer. Detector dark current data are subtracted from each acquired spectrum. Broadband tuning of the laser is accomplished using two Brewster-angle prisms and a movable slit effected by coordinated operation of two micrometers. As illustrated in Fig. 1, the resonator of the laser is isolated from the atmosphere to avoid atmospheric contributions to the absorption spectrum.

The plasma discharge is formed in a 1-in.-long copper

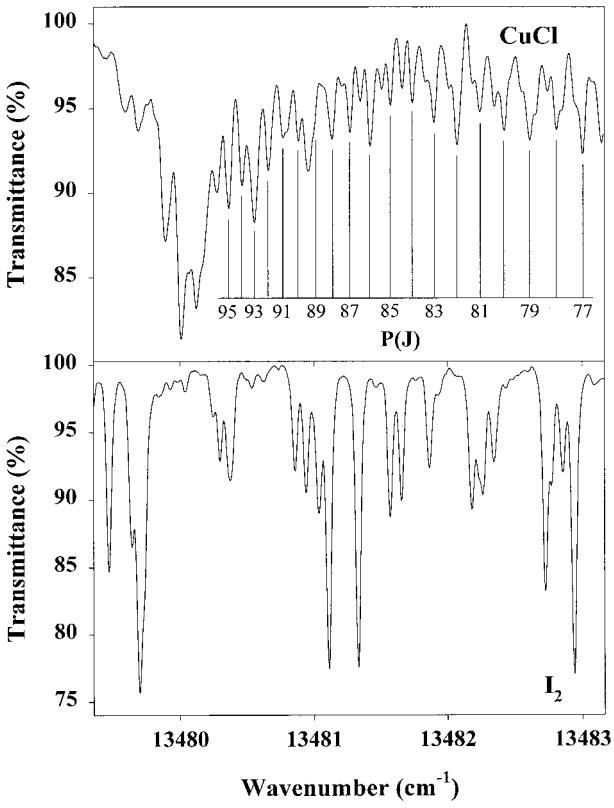

FIG. 2. The bandhead region of the (0, 0) band of the near-infrared spectrum of $^{65}Cu^{35}Cl$. The corresponding I_2 calibration spectrum is shown in the bottom panel.

hollow cathode from a flow of CCl_4 and Ar support gas. Argon is admitted at a rate of 10 sccm as fixed by a mass flow controller (MKS Model 247C). Restricted flow of vapor due to a needle valve at the inlet to the CCl_4 reservoir and a throttled flow of gas to the mechanical pump enable a pressure of approximately 25 mTorr of CCl_4 to be maintained at a total chamber pressure of 1.45 Torr. Pressures are measured by a 10-Torr capacitance manometer. The water-cooled hollow cathode is powered by an ENI DCG-100 DC Plasma generator, which serves as a digital power supply. It is operated at 740 V only for a brief period of time during the acquisition of CuCl spectra. Acquisition is initiated after the discharge current has decreased and stabilized to 0.5 A (about 10 s). Immediately following the acquisition of the spectrum obtained with the plasma operating, a background spectrum is obtained using identical conditions except that the voltage is switched off and the current is 0.0 A. Division of the two dark current corrected spectra yields the spectrum of the plasma species.

Spectra are recorded as a series of overlapping, $\sim$5-cm^{-1}-wide, spectral profiles. In this case, calibration is accomplished by alternatively measuring the spectrum of the intracavity plasma species and an I_2 absorption spectrum (e.g., see Fig. 2) recorded from a 0.75-m-long extracavity cell. In the latter case, the ILS spectral output serves as the broadband spectral source; the I_2 spectrum is obtained by dividing the spectrum obtained with I_2 present in the external cell with that obtained when I_2 is absent from the cell. The widely used Iodine Atlas (*15, 16*) is used as calibration source. To correct for small changes in the dispersion ($\leq$1.7%) of the spectrum across the diode array, spectra recorded from a 10-mm-thick étalon provide a source of equally spaced fringes. Peak positions (absorption peaks and fringe positions) are determined from the zero-crossing points of the first derivative spectra using Savitzky–Golay polynomial smoothing. This procedure enables positions to be determined with an accuracy of better than 0.002 cm^{-1}.

The intracavity compartment was not optimized for the hollow cathode (achieved by minimizing L with respect to l). However, as illustrated in the figures, spectra of good S/N are observed. Assuming the CuCl species are only observed inside the hollow cathode, an effective path length of 0.28 km is obtained for a t_g value of 80 μs. T_g values from 80 to 160 μs were employed. The hollow cathode is identical in geometry to the form used for observing emission in high-resolution FT measurements such as those made at the National Solar Observatory at Kitt Peak, Arizona.

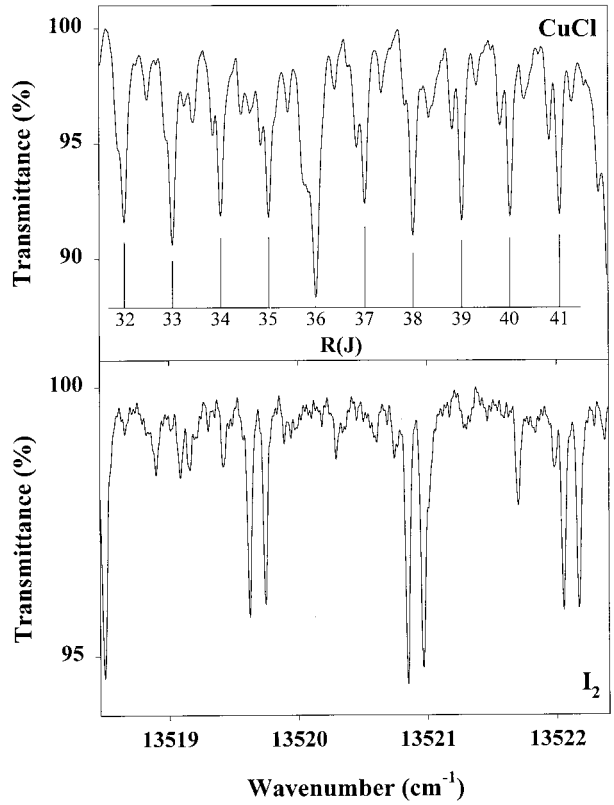

FIG. 3. A portion of R branch of the (0, 0) band of the near-infrared spectrum of $^{65}Cu^{35}Cl$. The bottom panel shows the corresponding I_2 calibration spectrum.

TABLE 1

Comparison of Calculated D_0' and D_0'' Values for Several Possible Rotational Assignments with the D_0' and D_0'' Values Predicted by the Kratzer Relationship (in cm^{-1})

Assignment label	D_0''	D_0'
R1	0.15×10^{-7}	-0.53×10^{-7}
R2	0.83×10^{-7}	0.15×10^{-7}
R3	0.15×10^{-6}	0.83×10^{-7}
R4	0.22×10^{-6}	0.15×10^{-6}
R5	0.28×10^{-6}	0.22×10^{-6}
Kratzer	0.13×10^{-6}	0.84×10^{-7}

TABLE 2

Molecular Constants (in cm^{-1}) for the Near-Infrared Transition of $^{63}Cu^{35}Cl$

	E_v	B_v	$D_v \times 10^7$	$H_v \times 10^{12}$
Lower State				
v=0	E	0.175926(12)	1.472(14)	-
v=1	E + 431.61(24)	0.174147(11)	1.542(13)	-
v=2	E + 853.72(32)	0.172346(17)	1.639(32)	-
Upper State				
v=0	E + 13506.8666(17)	0.176049(12)	0.840(13)	0.404(43)
v=1	E + 14026.94(24)	0.175092(11)	0.866(13)	0.390(23)
v=2	E + 14538.44(32)	0.174091(17)	0.893(30)	0.249(48)

Note. One standard deviation given in parentheses. The H'' values were too negligible to be determined by the fitting process.

RESULTS AND DISCUSSION

The near-infrared transition of CuCl was recorded from 13 450 to 13 750 cm^{-1}. The (0, 0), (1, 1), and (2, 2) bands were observed with rotational resolution. As shown in Fig. 2, the spectrum of the (0, 0) band is degraded to the violet with the bandhead occurring at relatively high J ($J > 80$). One strong P branch (see Fig. 2) and one strong R branch (see Fig. 3) were readily identified in each band. Peak positions for the (0, 0) band compare moderately well with those from the previous high-resolution analysis (*2*). The slight deviations in the peak positions (± 0.08 cm^{-1}) are probably due to the poorer precision and accuracy of the spectrograph used in the previous work.

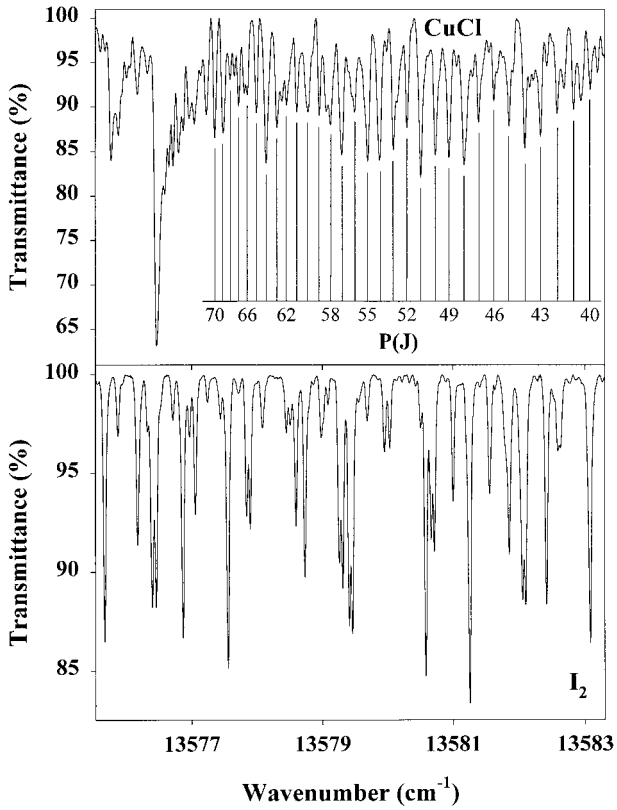

FIG. 4. The bandhead region of the (1, 1) band of the near-infrared spectrum of $^{65}Cu^{35}Cl$. Shown in the bottom panel is the corresponding I_2 calibration spectrum.

There are two copper isotopes ^{63}Cu and ^{65}Cu at 69.17 and 30.83% abundance, respectively, and two chlorine isotopes ^{35}Cl and ^{37}Cl at 75.77 and 24.23% abundance (*17*), respectively. Thus four CuCl isotopomers are possible: $^{63}Cu^{35}Cl$ (52.41%), $^{63}Cu^{37}Cl$ (23.36%), $^{65}Cu^{35}Cl$ (16.76%), and $^{65}Cu^{37}Cl$ (7.47%). Absorption peaks due to the $^{63}Cu^{35}Cl$ and $^{63}Cu^{37}Cl$ isotopomers are easily identified in Fig. 3, whereas the peaks associated with the $^{65}Cu^{35}Cl$ and $^{65}Cu^{37}Cl$ molecules are weak and are hidden by overlap with other stronger peaks. Only the $^{63}Cu^{35}Cl$ peak positions were used in the final fit.

Initially, we attempted to determine if the transition did (or did not) involve the $X^1\Sigma^+$ ground electronic state. Using the $^{63}Cu^{35}Cl$ microwave constants (*18*) to calculate the energy levels of the ground state, we determined the ground state ΔF_2 values (*19*) and concluded that the transition *does not* involve the ground state. From the structure of the electronic transition (one strong P branch and one strong R branch), we determined that the transition has $\Delta\Omega = 0$ symmetry. No Q branch was identifiable in any of the vibronic bands. We have fit the bands as Hund's case (c), $\Omega = 0$ states. However, some weak structure was observed near the origin area (and throughout the entire spectrum) which may or may not be due to this electronic transition of CuCl, so the symmetry of the electronic states is not definitive.

The (0, 0), (1, 1), and (2, 2) bands were initially fitted band by band to the standard energy level expression for an $\Omega = 0$ state (*19*) to produce a set of molecular constants for each vibronic level. Several possible rotational assignments were considered since low J lines were not observed. For each

TABLE 3

Line Positions, Assignments, and Residuals for the (3a) (0, 0) Vibronic Band, (3b) (1, 1) Vibronic Band, and (3c) (2, 2) Vibronic Band of the Near-Infrared Transition of $^{63}Cu^{35}Cl$

J″	P(J″)	o-c	R(J″)	o-c	J″	P(J″)	o-c	R(J″)	o-c
13	13502.321	0.007			55	13488.547	0.002	13527.514	-0.001
14	13501.957	-0.009			56	13488.258	0.003	13527.926	0.002
15	13501.617	-0.003			57	13487.970	0.001	13528.339	0.004
16	13501.272	0.000			58	13487.689	0.003	13528.755	0.005
17	13500.933	0.007			59	13487.411	0.007	13529.175	0.009
18	13500.573	-0.007			60	13487.131	0.004	13529.590	0.004
19	13500.234	-0.001			61	13486.853	0.000	13530.016	0.007
20	13499.897	0.007			62	13486.579	-0.003	13530.440	0.005
21	13499.560	0.014	13514.688	0.009	63	13486.311	-0.003	13530.860	-0.004
22	13499.214	0.012	13515.045	0.006	64	13486.049	-0.003	13531.295	-0.002
23	13498.862	0.003	13515.406	0.007	65	13485.787	-0.004	13531.732	-0.002
24	13498.511	-0.006	13515.759	-0.001	66	13485.534	-0.001	13532.170	-0.003
25	13498.170	-0.006	13516.118	-0.004	67	13485.281	-0.002	13532.618	0.002
26	13497.829	-0.007	13516.486	0.002	68	13485.032	-0.003	13533.064	0.000
27	13497.497	0.002	13516.851	0.004	69	13484.790	-0.001	13533.514	-0.001
28	13497.156	0.000	13517.214	0.003	70	13484.546	-0.006	13533.977	0.006
29	13496.820	0.001	13517.571	-0.005	71	13484.301	-0.016	13534.429	-0.001
30	13496.486	0.004	13517.942	0.002	72	13484.069	-0.017	13534.896	0.002
31	13496.150	0.005	13518.303	-0.004	73	13483.839	-0.022	13535.359	-0.004
32	13495.817	0.006	13518.668	-0.006	74	13483.629	-0.011	13535.833	-0.003
33	13495.479	0.002	13519.036	-0.006	75	13483.421	-0.003	13536.307	-0.006
34	13495.147	0.003	13519.406	-0.006	76	13483.213	0.000	13536.797	0.002
35	13494.813	0.000	13519.776	-0.006	77	13483.005	-0.002	13537.279	-0.004
36	13494.482	-0.001	13520.141	-0.013	78	13482.810	0.003	13537.773	-0.002
37	13494.151	-0.003	13520.520	-0.006	79	13482.611	-0.001		
38	13493.822	-0.005	13520.894	-0.007	80	13482.420	-0.003		
39	13493.499	-0.002	13521.272	-0.004	81	13482.239	-0.001		
40	13493.174	-0.002	13521.646	-0.006	82	13482.068	0.006		
41	13492.854	0.000	13522.028	-0.003	83	13481.894	0.004		
42	13492.530	-0.003	13522.401	-0.009	84	13481.732	0.006		
43	13492.210	-0.004	13522.791	-0.001	85	13481.569	0.002		
44	13491.891	-0.005	13523.174	-0.001	86	13481.417	0.002		
45	13491.572	-0.009	13523.562	0.002	87	13481.266	-0.004		
46	13491.263	-0.004	13523.949	0.003	88	13481.132	0.000		
47	13490.955	0.000	13524.339	0.005	89	13480.994	-0.007		
48	13490.647	0.002	13524.727	0.003	90	13480.879	0.003		
49	13490.340	0.001	13525.123	0.007	91	13480.765	0.005		
50	13490.036	0.003	13525.515	0.004	92	13480.656	0.005		
51	13489.735	0.005	13525.916	0.009	93	13480.551	0.002		
52	13489.436	0.005	13526.311	0.005	94	13480.460	0.004		
53	13489.141	0.008	13526.708	0.002	95	13480.362	-0.009		
54	13488.843	0.005	13527.109	-0.001	96	13480.273	-0.022		

possible assignment, the rotational constants were noted and the final assignment was determined when the centrifugal distortion constants, $D_{v'}$ and $D_{v''}$, for the fitted lines were consistent with the centrifugal distortion constants predicted by the Kratzer relationship (*19*). The fitted D'_0 and D''_0 values for several possible rotational assignments are given in Table 1 and the values predicted by the Kratzer relationship are presented in Table 1 for comparison. With respect to the original assignment by Balfour and Ram (*2*), the final rotational assignments are shifted by +3 in the *R* branch and −3 in the *P* branch (hence the "R3" label for the rotational assignment). A portion of the (1, 1) vibronic band near the bandhead is shown in Fig. 4.

Since only the (0, 0), (1, 1), and (2, 2) bands were recorded, the vibrational constants could not be determined directly from our data alone. The vibrational constants were obtained in the following manner. Using the rotational constants for $v' = 1$ and $v'' = 0$, the exact J'' value for the (1, 0) bandhead was determined, $J'' = 125$. The $P(124)$, $P(125)$, and $P(126)$ lines of the (1, 0) band were fitted to the bandhead position given by Rao and Rao (*1*). This yields a ground state vibrational frequency limited only by the accuracy of their spec-

TABLE 3—*Continued*

J″	P(J″)	o-c	R(J″)	o-c	J″	P(J″)	o-c	R(J″)	o-c
3			13596.744	-0.001	51	13580.507	0.000	13616.483	-0.001
4			13597.099	-0.004	52	13580.297	0.000	13616.972	0.004
5			13597.466	0.004	53	13580.093	0.002	13617.459	0.002
6			13597.815	-0.009	54	13579.888	-0.002	13617.955	0.006
7			13598.192	0.005	55	13579.694	0.002	13618.440	-0.006
8			13598.556	0.004	56	13579.490	-0.010	13618.938	-0.011
9			13598.915	-0.005	57	13579.298	-0.014	13619.442	-0.013
10	13591.936	0.001	13599.284	-0.005	58	13579.124	-0.005	13619.951	-0.014
11	13591.617	0.010	13599.645	-0.015	59	13578.957	0.006	13620.471	-0.010
12	13591.285	0.005	13600.036	0.002	60	13578.776	-0.002	13620.987	-0.014
13	13590.971	0.016	13600.410	0.001	61	13578.611	0.001	13621.511	-0.015
14	13590.644	0.012	13600.783	-0.003	62	13578.455	0.007	13622.037	-0.018
15	13590.307	-0.005	13601.159	-0.006	63	13578.309	0.019	13622.598	0.007
16	13589.990	-0.003	13601.542	-0.004	64	13578.142	0.003	13623.131	0.000
17	13589.679	0.002	13601.925	-0.004	65	13577.991	-0.001	13623.676	-0.001
18	13589.355	-0.007	13602.313	-0.002	66	13577.853	0.002	13624.224	-0.004
19	13589.046	-0.005	13602.704	0.001	67	13577.720	0.003	13624.774	-0.011
20	13588.731	-0.010	13603.099	0.007	68	13577.588	0.000	13625.320	-0.028
21	13588.426	-0.007	13603.490	0.005	69	13577.475	0.009	13625.878	-0.038
22	13588.124	-0.004	13603.882	0.003	70	13577.355	0.007	13626.457	-0.034
23	13587.816	-0.009	13604.271	-0.004	71	13577.239	0.000	13627.033	-0.038
24	13587.516	-0.008	13604.673	-0.001	72	13577.142	0.007	13627.614	-0.043
25	13587.214	-0.013	13605.079	0.004	73	13577.044	0.006	13628.212	-0.038
26	13586.927	-0.004	13605.484	0.006	74	13576.959	0.011	13628.813	-0.036
27	13586.628	-0.009	13605.890	0.007	75	13576.865	0.001	13629.449	-0.006
28	13586.348	0.001	13606.299	0.008	76	13576.787	-0.001	13630.068	0.000
29	13586.056	-0.004	13606.706	0.004	77	13576.717	-0.001	13630.683	-0.004
30	13585.779	0.005	13607.116	0.000	78	13576.649	-0.008	13631.314	0.000
31	13585.494	0.003	13607.534	0.003	79	13576.595	-0.008	13631.949	0.001
32	13585.207	-0.005	13607.954	0.004	80	13576.550	-0.006	13632.585	-0.004
33	13584.933	-0.002	13608.375	0.004	81	13576.475	-0.042	13633.246	0.008
34	13584.667	0.006	13608.798	0.002	82	13576.475	-0.011	13633.912	0.017
35	13584.390	0.001	13609.222	0.000	83			13634.565	0.006
36	13584.124	0.002	13609.659	0.007	84			13635.225	-0.006
37	13583.856	-0.001	13610.090	0.006	85			13635.918	0.006
38	13583.597	0.002	13610.525	0.006	86			13636.609	0.009
39	13583.341	0.005	13610.960	0.002	87			13637.309	0.012
40	13583.084	0.003	13611.405	0.005	88			13638.014	0.011
41	13582.833	0.004	13611.854	0.010	89			13638.715	-0.002
42	13582.585	0.005	13612.300	0.007	90			13639.444	0.003
43	13582.328	-0.007	13612.743	-0.001	91			13640.158	-0.015
44	13582.093	0.000	13613.203	0.004	92			13640.915	-0.001
45	13581.853	-0.002	13613.650	-0.007	93			13641.671	0.004
46	13581.624	0.004	13614.111	-0.008	94			13642.423	-0.005
47	13581.391	0.001	13614.585	0.001	95			13643.193	-0.006
48	13581.172	0.009	13615.050	-0.003	96			13643.976	-0.004
49	13580.938	-0.003	13615.526	0.000	97			13644.766	-0.006
50	13580.732	0.010	13616.007	0.005	98			13645.576	0.002

trometer, ~0.4 cm^{-1}. This same procedure was used also for the (2, 1) band.

A combined fit of all three vibronic bands of the near-infrared electronic transition of CuCl produced a set of 21 molecular constants, which are presented in Table 2. The average uncertainty of the individual rotational lines as determined from the standard deviation of the fit is 0.005 cm^{-1}, which is consistent with the estimated measurement accuracy. The observed rotational lines, assignments, and fit residuals are presented in Table 3.

The data were also fitted in a nonlinear least-squares program that incorporated Dunham-type vibronic energy expressions (*20*). The 14 Dunham-type constants required to fit the data are presented in Table 4. Literature values are presented also in Table 4 for comparison. Significant differences from the values determined by Rao and Rao (*1*) are observed. In their

TABLE 3—*Continued*

J″	P(J″)	o-c	R(J″)	o-c	J″	P(J″)	o-c	R(J″)	o-c
9			13688.367	0.010	51	13672.168	0.002	13707.929	-0.003
10			13688.740	-0.001	52	13672.043	-0.001	13708.501	0.000
11			13689.126	-0.002	53	13671.935	0.006	13709.068	-0.009
12			13689.514	-0.004	54	13671.824	0.004	13709.646	-0.012
13			13689.908	-0.004	55	13671.720	0.003	13710.245	0.000
14			13690.318	0.009	56	13671.633	0.012	13710.837	-0.001
15			13690.726	0.015	57	13671.544	0.012	13711.442	0.003
16			13691.114	-0.001	58	13671.451	0.002	13712.043	-0.002
17	13679.368	0.026	13691.520	-0.004	59	13671.368	-0.004	13712.664	0.007
18	13679.076	0.017	13691.935	-0.002	60	13671.290	-0.013	13713.276	-0.001
19	13678.789	0.009	13692.352	-0.001	61	13671.234	-0.006	13713.907	0.004
20	13678.497	-0.006	13692.761	-0.012	62			13714.543	0.007
21	13678.222	-0.010	13693.185	-0.012	63			13715.179	0.003
22	13677.966	0.002	13693.634	0.010	64			13715.819	-0.004
23	13677.701	0.000	13694.059	0.003	65			13716.480	0.003
24	13677.441	0.000	13694.505	0.014	66			13717.127	-0.012
25	13677.193	0.008	13694.931	0.000	67			13717.809	0.001
26	13676.926	-0.008	13695.382	0.008	68			13718.470	-0.014
27	13676.675	-0.012	13695.819	-0.003	69			13719.165	-0.003
28	13676.444	0.001	13696.275	0.001	70			13719.876	0.015
29	13676.209	0.005	13696.701	-0.028	71			13720.558	-0.003
30	13675.972	0.002	13697.173	-0.017	72			13721.279	0.009
31	13675.745	0.005	13697.649	-0.004	73			13721.976	-0.010
32	13675.519	0.005	13698.114	-0.008	74			13722.712	0.001
33	13675.298	0.004	13698.579	-0.016	75			13723.456	0.011
34	13675.078	0.001	13699.070	-0.002	76			13724.192	0.005
35	13674.863	-0.002	13699.543	-0.012	77			13724.939	0.001
36	13674.661	0.003	13700.042	0.001	78			13725.701	0.003
37	13674.451	-0.005	13700.535	0.003	79			13726.457	-0.010
38	13674.258	0.000	13701.030	0.002	80			13727.244	-0.002
39	13674.071	0.006	13701.538	0.010	81			13728.038	0.005
40	13673.888	0.011	13702.057	0.024	82			13728.825	-0.006
41	13673.688	-0.008	13702.559	0.015	83			13729.635	-0.003
42	13673.504	-0.014	13703.054	-0.005	84			13730.458	0.004
43	13673.342	-0.004	13703.575	-0.004	85			13731.287	0.004
44	13673.178	0.000	13704.104	0.000	86			13732.108	-0.012
45	13673.000	-0.017	13704.642	0.007	87			13732.965	-0.002
46	13672.850	-0.011	13705.197	0.027	88			13733.836	0.009
47	13672.706	-0.004	13705.717	0.005	89			13734.696	0.000
48	13672.565	-0.001	13706.260	0.001	90			13735.567	-0.008
49	13672.446	0.020	13706.814	0.003	91			13736.470	0.002
50	13672.320	0.027	13707.374	0.005	92			13737.375	0.004

vibrational analysis, only bandheads were used. However, although the rotational constants of the two electronic states are very close in value, the centrifugal distortion constants are very different, consequently there is considerable change in the J value of the P branch at each bandhead. For example, the (0, 0) bandhead is at $P(\sim 100)$; the (1, 1) bandhead is at $P(\sim 85)$; the (2, 2) bandhead is at $P(\sim 70)$; the (1, 0) bandhead is at $P(\sim 125)$, and the (2, 1) bandhead is at $P(\sim 107)$. This also explains the lack of data for the $\Delta v = 2$ progression (*1*): based on the molecular constants, the (2, 0) band does not form a bandhead. The bands of the next sequence, $\Delta v = 3$, are expected to be red-degraded, and these bands may account for some of the unidentified bands observed in the red region by Rao (*10*).

We have considered all the known electronic states for CuCl as possible states involved in the near-infrared transition. A comparison of selected molecular constants of the known electronic states of CuCl is given in Table 5. The molecular constants of the two states involved in the near-infrared transition clearly do not match any of the constants of the known electronic states. Although it is possible that the lower state of the near-infrared bands might be the $a^3\Sigma_0^+$ state, it is unlikely that the molecular constants of the $a^3\Sigma_0^+$ and $a^3\Sigma_1^+$ components would have such different molecular constants. In addi-

tion, there are no known or predicted electronic states near 32 263 cm^{-1} (*9*).

It is informative to look at the information available on the electronic structure of CuCl. The ground state has a $Cu^+(3d^{10})Cl^-(3p^6)$ electronic configuration, and all the previously observed excited electronic states (between 19 000 and 26 000 cm^{-1}) arise from the $Cu^+(3d^9 4s^1)Cl^-(3p^6)$ electronic configuration (*6–9*). The excited state term energies compare well with the Cu^+ atomic excited state term energies further supporting this model of the bonding; the excited $Cu^+(3d^9 4s^1)$ atomic ^3D and ^1D states are located 23 000 and 26 000 cm^{-1} above the ground state (*21*). Recent *ab initio* calculations have studied the excited "neutral" $Cu(3d^{10}4s^1)Cl(3p^5)$ states (*9*). The neutral states are calculated to be 45 000–55 000 cm^{-1} above the ground state. However, these are expected to have significantly longer bond lengths than the ionic states (*9*), and thus are not good candidates for states involved in the near-infrared transition.

Based on the Cu^+ atomic electronic transitions (*21*), numerous excited molecular electronic states of CuCl are anticipated to occur in the 60 000–75 000 cm^{-1} region dominated by the $Cu^+(3d^9 4p^1)Cl^-(3p^6)$ and $Cu^+(3d^8 4s^2)Cl^-(3p^6)$ electronic configurations. Although it is simply speculative at this point, this manifold of electronic states could host the unknown excited electronic states of the near-infrared transition.

CONCLUSIONS

The (0, 0), (1, 1), and (2, 2) vibronic bands of the near-infrared transition of CuCl were observed by intracavity laser absorption spectroscopy. A rotational analysis of these vibronic bands yielded new molecular constants for the two states involved in the near-infrared transition. Based on the molecular constants, this transition does not connect to the $X^1\Sigma^+$ ground state, but occurs between two unknown excited states.

More generally, intracavity laser absorption spectroscopy has been shown to be an effective technique for the acquisition of high-resolution, Doppler-limited spectra of gas-phase radicals.

TABLE 4
Dunham-type Molecular Constants for the Near-Infrared Transition of $^{63}Cu^{35}Cl$

	Lower State	Upper State	Lit. Value (1) (Lower, Upper)
T_e	E	E + 13462.9736(23)	0.0, 13434.1
ω_e	441.43(13)	528.9834(13)	415.8, 509.1
$\omega_e x_e$	4.975(29)	4.519(29)	1.09, 1.47
B_e	0.1768498(98)	0.1765576(99)	
$\alpha_e \times 10^3$	1.8068(44)	0.9760(46)	
$\gamma_e \times 10^5$		-0.543(27)	
$D_e \times 10^7$	1.4739(76)	0.8603(86)	
$\beta_e \times 10^8$	-0.4622(78)		
$H_e \times 10^{12}$		0.352(17)	
r_e (X)	2.05922(6)	2.06093(6)	

Note. One standard deviation given in parentheses.

TABLE 5
Comparison of the Molecular Constants of Different Electronic States of $^{63}Cu^{35}Cl$

	Original Assignments [a]	T_0	B_0	$\nu_{1\leftarrow 0}$
$X\,^1\Sigma^+$	$X\,^1\Sigma^+$	0.0	0.177741294(4)	414.4191(28)
$a\,^3\Sigma^+_0$		18800.[b]		
$a\,^3\Sigma^+_1$	$A\,^1\Pi$	18994.4565(14)	0.1701869(17)	405.8[c]
$b\,^3\Pi_1$	$B\,^1\Pi$	20476.1021(20)	0.1697634(15)	398.2761(25)
$b\,^3\Pi_0$	$C\,^1\Sigma^+$	20621.8425	0.170659	396.093
$A\,^1\Pi$	$D\,^1\Pi$	22958.4770(12)	0.1688536(14)	391.5108(30)
$B\,^1\Sigma^+$	$E\,^1\Sigma^+$	23068.2615(27)	0.1676150(47)	402.2314(30)
$c\,^3\Delta_1$	$F\,^1\Pi$	25477.36(5)[d]	0.1603(5)[d]	381.64(5)[d]
NIR Band, Lower state		E	0.175926(12)	431.61(24)
NIR Band, Upper state		E + 13462.9736(17)	0.176049(12)	520.07(24)

Note. Literature values are from Ref. (*11*), except where noted.
[a] From Huber and Herzberg (*22*).
[b] The spin-spin coupling constant for the $a^3\Sigma^+$ state is calculated to be λ = 97 cm^{-1} (*8*).
[c] From Ref. (*10*).
[d] From Ref. (*23*).

ACKNOWLEDGMENTS

Partial support for this work was provided by the National Science Foundation, through Grant No. NSF-CHE-9753254, and from a Research Award by the University of Missouri-St. Louis.

REFERENCES

1. P. M. R. Rao and P. R. Rao, *Spectrosc. Lett.* **7,** 463–468 (1974).
2. W. J. Balfour and R. S. Ram, *J. Phys. B* **17,** L19–L21 (1984).
3. E. L. Manson, F. C. DeLucia, and W. Gordy, *J. Chem. Phys.* **62,** 1040–1043 (1975).
4. F. Ahmed, R. F. Barrow, A. H. Chojnicki, C. Dufour, and J. Schamps, *J. Phys. B* **15,** 3801–3818 (1982).
5. J. M. Delaval, Y. Lefebvre, H. Bocquet, P. Bernage, and P. Niay, *Chem. Phys.* **111,** 129–136 (1987).
6. N. W. Winter and D. L. Huestis, *Chem. Phys. Lett.* **133,** 311–316 (1987).
7. J. M. Delaval, J. Schamps, A. Ramirez-Solis, and J. P. Daudey, *J. Chem. Phys.* **97,** 6588–6592 (1992).
8. C. Sousa, W. A. de Jong, R. Broer, and W. C. Nieuwpoort, *J. Chem. Phys.* **106,** 7162–7169 (1997).
9. C. Sousa, W. A. de Jong, R. Broer, and W. C. Nieuwpoort, *Mol. Phys.* **92,** 677–686 (1997).

10. P. M. R. Rao, *Indian J. Pure Appl. Phys.* **18,** 200–203 (1980).
11. T. Parekunnel, T. Hirao, P. F. Bernath, M. Elhanine, T. L. Kellerman, and L. C. O'Brien, unpublished manuscript.
12. N. Sadeghi, I. Hikmet, I. Colomb, and D. W. Setser, *Chem. Phys.*, in press.
13. B. Kalmar and J. J. O'Brien, *J. Mol. Spectrosc.* **192,** 386–393 (1998).
14. J. Sieks, T. Latz, V. M. Baev, and P. E. Toschek, "Proceedings of the 1996 European Quantum Electronics Conference (EQEC'96)," p. 100, QWB6, Hamburg, Germany, 8–13 September 1996.
15. S. Gerstenkorn, J. Verges, and J. Chevillard, *in* "Atlas du Spectre d'Absorption de la Molecule d'Iode, Vol. III. 11,000–14,000 cm^{-1}," Laboratoire Aimé Cotton, CNRS II, Orsay, 1982.
16. S. Gerstenkorn and P. Luc, *J. Phys.* **46,** 867–881 (1985).
17. "Handbook of Chemistry and Physics," 71st ed., CRC Press Inc., Boston, 1990.
18. K. D. Hensel, C. Styger, W. Jäger, A. J. Merer, and M. C. L. Gerry, *J. Chem. Phys.* **99,** 3320–3328 (1993).
19. G. Herzberg, "Spectra of Diatomic Molecules," Van Nostrand–Reinhold, New York, 1950.
20. Peter F. Bernath, "Spectra of Atoms and Molecules," Oxford Univ. Press, London, 1995.
21. C. E. Moore, "Atomic Energy Levels," NSRDS-NBS 35, 1975.
22. K.-P. Huber and G. Herzberg, "Constants of Diatomic Molecules," Van Nostrand–Reinhold, New York, 1975.
23. P. R. Rao, R. K. Asundi, and J. K. Brody, *Can. J. Phys.* **40,** 412–422 (1962).